

AN ANALYTICAL ESTIMATE OF SHEAR BAND INITIATION IN A NECKED BAR

T. IWAKUMA and S. NEMAT-NASSER

Northwestern University, Evanston, IL 60201, U.S.A.

(Received 20 October 1980; in revised form 20 April 1981)

Abstract—The initiation of localized deformation in the form of shear bands within the necked region of an axially loaded rectangular specimen is studied analytically for a plane strain deformation. A semi-inverse method is used to estimate the nonhomogeneous stress state in the necked region prior to shear band inception. For the localization analysis a generalized J_2 plasticity theory which includes the dilatancy and pressure sensitivity effects is employed. The analytical estimates are compared with some existing experimental results, and good correlation is obtained.

1. INTRODUCTION

It is known that uniaxial extension of thin metal sheets may lead to necking and then to the formation of localized shear bands within the necked region; see, e.g. Weinrich and French[1], and Anand and Spitzig[2]. The state of stress in the necked region prior to the inception of shear bands is nonhomogeneous, and therefore a complete description of the deformation history requires a numerical approach. An analysis of this kind recently has been performed by Tvergaard *et al.*[3] for a plane strain extension of a finite rectangular bar, using several constitutive relations. While an approach of this kind provides complete information of the deformation history, it requires extensive numerical calculations involving finite-element schemes with several thousand degrees of freedom. Another approach which has been extensively used, is to assume a homogeneous state of stress prior to the inception of shear bands, and then within the theoretical framework given by Hill[4] seek to obtain conditions under which the governing field equations for the rate of deformation from the given homogeneous state cease to be elliptic. The resulting characteristics then delineate possible shear band orientations. Calculations of this kind are found in the work by Hill and Hutchinson[5], Rice[6], Stören and Rice[7], Rudnicki and Rice[8], Hutchinson and Neale[9], Knowles and Sternberg[10], Needleman[11], and Nemat-Nasser[12].

In the uniaxial extension of a rectangular bar it is known that deviation by diffused necking from a homogeneous deformation state is possible while the rate field equations are elliptic, i.e. before localized deformation by shear bands becomes possible; Hill and Hutchinson[5]. Moreover, the assumption that shear bands are initiated in thin sheets directly from a homogeneous state without a prior diffused necking, is not borne out by experimental results (see, e.g. Weinrich and French[1]).

In this work bifurcation in the form of localized shear bands from the nonhomogeneous stress and deformation state in the necked region of a tensile specimen deformed under plane strain conditions, is examined. To this end the profile of the necked portion of the specimen is expanded in a Fourier series with unknown coefficients. These coefficients may be fixed by comparing certain overall average deformation measures and the conjugate forces with the corresponding quantities obtained experimentally. In this work a three-term series approximation is used.

For a given shape of necked portion a statically admissible stress field is obtained which satisfies exactly the equilibrium equations and the free stress boundary conditions on the lateral surfaces of the necked specimen. In addition, the obtained overall stress field is made to satisfy the overall equilibrium, i.e. conditions at infinity.

With the nonhomogeneous stress field established, bifurcation analysis is performed within the framework given by Hill[4], where the characteristics are no longer straight lines. For the representation of the material, a generalized J_2 plasticity theory which includes dilatancy and pressure sensitivity effects is used, and the minimum value of the overall applied stress which is required to yield real characteristics at each point in the necked region, together with the corresponding characteristic directions, is estimated. The results are compared with experi-

ments by Anand and Spitzig[2], and good correlation is obtained. It turns out that the incipience of shear band formation is highly dependent on the material parameters. The critical value of the stress at which the shear band formation first becomes possible is not significantly affected by the shape of the necked region. On the other hand, the location of the shear band initiation critically depends on the shape of the neck and possible imperfections. These results are consistent with the numerical results of Tvergaard *et al.*[3].

2. STATEMENT OF PROBLEM

Consider bifurcation in the form of localized shear bands from a nonhomogeneous state of deformation in the necked region of a thin sheet under uniaxial tension. The objective is to calculate the critical value of the axial stress at which a shear band can initiate at a point within the necked region. It is assumed that such a critical load coincides with the minimum value of the stress at which the rate field equations for the first time yield real characteristics, these characteristics defining the shear band directions.

To this end first a statically admissible stress field is obtained analytically for an arbitrary but suitably smooth necked profile under a plane strain condition. Then the necked profile is represented in the form of a Fourier series and the corresponding coefficients are adjusted from the knowledge of the overall average deformation parameters and the corresponding overall forces. For example, if a two-term Fourier expansion is used, then the overall stretch and the corresponding average axial stress are sufficient to fix the needed parameters. Since in theoretical investigations, the constitutive parameters such as the tangent modulus and the work-hardening parameter are usually fixed on the basis of a uniaxial stress-strain relation and often on the assumption of a power law connecting the effective stress with the effective strain, the above approach seems reasonable. At any rate, if a deformation theory is involved, then the necked profile can be approximated to any degree of accuracy by estimating a suitable number of Fourier coefficients in its series expansion. In the present work, however, attention is confined to a three-term approximation only.

The calculation of the critical axial stress and of the characteristic directions is done within Hill's[4] general theory where, because of the nonhomogeneous state of deformation and stress, the characteristics are no longer straight lines.

Consider a fixed rectangular Cartesian coordinate system with coordinate axes x_i , $i = 1, 2, 3$, and let $\dot{\tau}_{ij}$ be the rate of change of the *nominal* stress, referred to and measured per unit current area. For a general class of rate-independent materials, $\dot{\tau}_{ij} = C_{ijkl}v_{k,l}$, where v_k is the velocity field and C_{ijkl} depends among other things on the current stress state, but is independent of the rates; here and in the sequel repeated indices are summed, and comma followed by an index denotes partial differentiation with respect to the corresponding coordinate. In the absence of body forces, the rate differential equations for equilibrium are

$$\dot{\tau}_{ij,j} = [C_{ijkl}v_{k,l}]_{,j} = C_{ijkl}v_{k,lj} + C_{ijkl,j}v_{k,l} = 0. \quad (2.1)$$

It is clear from (2.1) that the loss of ellipticity can be decided from the structure of the matrix coefficient C_{ijkl} , which in general may vary from point to point within the necked region of the specimen in accordance with the variation of the stress and other field quantities. In this work rate constitutive relations based on a generalized J_2 theory are used to estimate the matrix C_{ijkl} , and the critical stress and the corresponding shear band directions are calculated for several combinations of material parameters.

3. CALCULATION OF STRESS FIELD

Let the x_1, x_2 -plane coincide with the middle plane of a necked thin sheet which is pulled in plane strain by axial stress, σ_0 , applied in the x_1 -direction; see Fig. 1. The necking has occurred in the region $|x_1| \leq l$, where the necked profile in the x_1, x_3 -plane is characterized by $x_3 = H(x_1)$, H being a suitably smooth function such that

$$H(\pm l) = H_0, \quad H'(\pm l) = 0, \quad (3.1)$$

where prime denotes differentiation. In Fig. 1, $\delta = (1/2)[H_0 - H(0)]$.

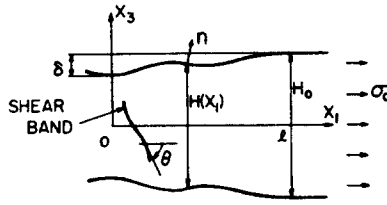


Fig. 1. A necked profile of a thin sheet in uniaxial extension.

With σ_{ij} being the Cauchy stress components, for the plane strain condition set

$$[\sigma_{12} \equiv 0, \sigma_{23} \equiv 0], \quad \sigma_{22} \equiv \frac{1}{2}(\sigma_{11} + \sigma_{33}), \quad (3.2)$$

where the appropriate expression for σ_{22} is given later on in relation to the considered rate constitutive relations; see (5.10').

Let $\mathbf{n}(\mathbf{x})$ be the exterior unit normal on the upper surface, S , of the necked region,

$$n_1(x_1) = \frac{-H'(x_1)/2}{\sqrt{1+(H'/2)^2}}, \quad n_2(x_1) = \frac{1}{\sqrt{1+(H'/2)^2}}. \quad (3.3)$$

The equilibrium equations throughout the bar and the boundary conditions on S , respectively, are

$$\begin{aligned} \sigma_{11,1} + \sigma_{31,3} &= 0, \\ \sigma_{13,1} + \sigma_{33,3} &= 0, \end{aligned} \quad (3.4)$$

and

$$\begin{aligned} \sigma_{11}n_1 + \sigma_{31}n_3 &= 0, \\ \sigma_{13}n_1 + \sigma_{33}n_3 &= 0, \quad \text{on } S. \end{aligned} \quad (3.5)$$

Let σ_0 be the overall applied stress in the x_1 -direction. The conditions at $x_1 = \pm l$ are

$$\sigma_{11}(\pm l) = \sigma_0, \quad \sigma_{13}(\pm l) = 0, \quad (3.6)$$

and the overall equilibrium requires

$$\int_{-H/2}^{+H/2} \sigma_{11} dx_3 = \sigma_0 H_0 \quad \text{for all } x_1. \quad (3.7)$$

In view of assumed symmetry with respect to the x_1, x_2 -plane, a reasonable approximation to the stress field is

$$\begin{aligned} \sigma_{11} &= a(x_1)(x_3)^2 + b(x_1), \\ \sigma_{33} &= c(x_1)(x_3)^4 + d(x_1), \\ \sigma_{13} &= e(x_1)(x_3)^3 + f(x_1)x_3, \end{aligned} \quad (3.8)$$

where coefficients a to f are functions of x_1 and are to be determined in such a manner that equilibrium conditions (3.4)–(3.7) are identically satisfied (a semi-inverse analytical approach). Therefore, (3.8) are substituted into (3.4) and (3.5) and upon integration and some manipulation, and in view of (3.6), (3.7), and symmetry conditions such as

$$b(x_1) = b(-x_1), \quad (3.9)$$

one arrives at

$$\begin{aligned}
 a(x_1) &= 12\sigma_0 \frac{H_0 - H}{H^3}, & b(x_1) &= \sigma_0, \\
 c(x_1) &= \sigma_0 \left(\frac{H_0 - H}{H^3} \right)''', & d(x_1) &= \frac{\sigma_0}{16} \{H(3H_0 - H)\}''', \\
 e(x_1) &= -4\sigma_0 \left(\frac{H_0 - H}{H^3} \right)', & f(x_1) &= 0.
 \end{aligned} \tag{3.10}$$

Equations (3.8) and (3.10) now provide the following statically admissible stress field for any suitably smooth shape function $H(x_1)$:

$$\begin{aligned}
 \frac{\sigma_{11}}{\sigma_0} &= 1 + 12 \frac{H_0 - H}{H} \left(\frac{x_3}{H} \right)^2, \\
 \frac{\sigma_{33}}{\sigma_0} &= \frac{1}{16} \{ (3H_0 - 2H)H'' - 2(H')^2 \} + \left\{ 6(H')^2 \frac{2H_0 - H}{H} - H''(3H_0 - 2H) \right\} \left(\frac{x_3}{H} \right)^4, \\
 \frac{\sigma_{13}}{\sigma_0} &= 4H' \frac{3H_0 - 2H}{H} \left(\frac{x_3}{H} \right)^3.
 \end{aligned} \tag{3.11}$$

4. SHAPE OF NECK AND AVERAGE STRAIN

For diffused suitably smooth necking in a bar, in view of symmetry the shape of the neck profile can be expressed by a Fourier cosine series,

$$H(x_1) = \sum_k C_k \cos \frac{k\pi x_1}{l}. \tag{4.1}$$

In the present work only a three-term approximation is considered,

$$\frac{H}{H_0} = 1 - \zeta \left(\cos \frac{\pi x_1}{l} + 1 \right) - \xi \left(1 - \cos \frac{2n\pi x_1}{l} \right), \tag{4.2}$$

where n is an integer, and

$$\zeta = \frac{\delta}{H_0}, \quad \delta = \frac{1}{2} [H_0 - H(0)]. \tag{4.3}$$

Note that (4.2) represents the assumed necked profile, and is not intended to characterize an initial imperfection. In the illustrative example which will follow, the integer n is used as a parameter that characterizes possible initial imperfections that have led to the necked profile of the kind represented by (4.2). The coefficients ζ and ξ are, however, functions of overall deformation and are to be determined by the consideration of the overall stress, deformation-relation.

Let H_0 be the thickness of the sheet just prior to diffused necking instability. It is assumed that the thickness outside of the necked region remains constant as necking develops and leads to the inception of a shear band. If L is the gauge length prior to necking and l is the corresponding length just at the inception of shear bands, the condition of incompressibility (if used) requires

$$LH_0 = \int_0^l H(x_1) dx_1. \tag{4.4}$$

Substitution from (4.2) into (4.4) yields

$$\lambda_{NH} = 1 + \epsilon_{NH} = \frac{l}{L} = \frac{1}{1 - \zeta - \xi}, \tag{4.5}$$

where λ_{NH} and ϵ_{NH} are the average stretch and elongation of the nonhomogeneous necked region, measured relative to the homogeneous configuration at the inception of diffused necking. To calculate the total stretch, λ_t , let the initial gauge length be l_i . Then

$$\lambda_t = \frac{l}{l_i} = \frac{L}{l_i} \frac{l}{L} = \lambda_H \lambda_{NH}, \quad (4.6)$$

where λ_H is the stretch just before necking. If a parametric study is made using ζ and ξ as parameters, then (4.5) and (4.6) yield the resulting stretches. From these stretches the overall average stress can be estimated from the experimental stress, strain-relation. If more than a uniaxial average stress, strain-relation is available, then the calculation of the state of stress and deformation in the necked region can be accordingly refined. For example, one may use a variational approach, and treat the Fourier coefficients in (4.1) as generalized coordinates. In the sequel ζ and ξ are treated as parameters defining the necked profile prior to shear band formation.

5. RATE CONSTITUTIVE RELATIONS

As a generalized J_2 plasticity theory which includes dilatancy and pressure effects consider the theory recently developed by Nemat-Nasser and Shokooh[13], which involves the following yield function and flow potential:

$$\begin{aligned} \text{Yield Function:} \quad & f \equiv \bar{\sigma} - F(I, \Delta, \bar{\epsilon}), \\ \text{Flow Potential:} \quad & g \equiv \bar{\sigma} + G(I, \Delta, \bar{\epsilon}), \end{aligned} \quad (5.1)$$

where

$$\begin{aligned} \bar{\sigma}^2 &= \frac{1}{2} \sigma'_{ij} \sigma'_{ij}, & I &= \sigma_{kk}, \\ \Delta &= \int_0^\theta \frac{\rho_0}{\rho} D_{kk}^p d\theta, & \bar{\epsilon} &= \int_0^\theta (2D_{ij}^p D_{ij}^p)^{1/2} d\theta. \end{aligned} \quad (5.2)$$

Here prime denotes the deviatoric part, superposed p stands for the plastic part, ρ and ρ_0 are the current and reference mass densities, respectively, Δ is the total plastic volumetric change measured with respect to the reference configuration, and $\bar{\epsilon}$ is the total effective plastic distortion; in (5.2), θ stands for a monotone increasing load parameter. The contribution to the total deformation rate tensor by the elastic distortion is characterized by an isotropic relation which connects the Jaumann rate of Cauchy stress,

$$\sigma_{ij}^0 = \dot{\sigma}_{ij} - W_{ik} \sigma_{kj} - W_{jk} \sigma_{ki}, \quad (5.3)$$

to the elastic part of the deformation rate tensor, D_{ij}^e , by

$$D_{ij}^e = \frac{1}{4\mu} (\delta_{ik} \delta_{jl} + \delta_{il} \delta_{jk}) \dot{\sigma}'_{kl} + \frac{1}{3\kappa} \delta_{ij} \delta_{kl} \frac{\dot{\sigma}'_{kl}}{3}, \quad (5.4)$$

where μ and κ are some appropriate shear and bulk moduli, W_{ij} being the spin tensor.

The contribution to the deformation rate by plastic distortion is obtained from (5.1),

$$D_{ij}^p = \frac{1}{H} \left(\frac{\sigma'_{ij}}{2\bar{\sigma}} + \frac{\partial G}{\partial I} \delta_{ij} \right) \left(\frac{\sigma'_{kl}}{2\bar{\sigma}} - \frac{\partial F}{\partial I} \delta_{kl} \right) \dot{\sigma}'_{kl}, \quad (5.5)$$

where H is the work-hardening parameter (this should not be confused with the neck profile),

$$H = 3 \frac{\rho_0}{\rho} \frac{\partial G}{\partial I} \frac{\partial F}{\partial \Delta} + \frac{\partial F}{\partial \bar{\epsilon}}, \quad (5.6)$$

and $(\partial G/\partial I)$ and $-(\partial F/\partial I)$ are the dilatancy and the pressure-sensitivity factors, respectively.

Equation (5.5) yields a plastic rate of deformation tensor coaxial with the stress tensor. It is commonly argued that the existence of microscopic slips and microscopic localized deformations may result in noncoaxiality. The corner theories of plasticity are motivated for this reason; see, e.g. Christoffersen and Hutchinson[14]. However, although a corner provides noncoaxiality, noncoaxiality can exist with smooth flow potentials. One way to account for this is to consider a contribution to the plastic distortion which is work-less and therefore makes no contribution to the rate of plastic energy loss. A term of this kind emerges naturally in the double-slip theory of granular materials; see, e.g. Mandel[15], Spencer[16, 17], Mehrabadi and Cowin[18, 19], Christoffersen *et al.*[20], and Nemat-Nasser *et al.*[21]. A similar contribution to the plastic strain rate has been considered on the basis of a deformation-type theory by Rudnicki and Rice[8], and Stören and Rice[7]. Following this line of thinking, (5.5) is modified to read

$$D_{ij}^p = \frac{1}{H} \left(\frac{\sigma'_{ij}}{2\bar{\sigma}} + \frac{\partial G}{\partial I} \delta_{ij} \right) \left(\frac{\sigma'_{kl}}{2\bar{\sigma}} - \frac{\partial F}{\partial I} \delta_{kl} \right) \dot{\sigma}_{kl} + A \left\{ \dot{\sigma}'_{ij} - \frac{1}{2\bar{\sigma}^2} \sigma'_{kl} \dot{\sigma}_{kl} \sigma'_{ij} \right\}, \quad (5.7)$$

where A is a compliance, type parameter that may depend on the deformation history; here $1/A$ is not necessarily a secant modulus.

Since $D_{ij} = D_{ij}^e + D_{ij}^p$ exactly, see Nemat-Nasser[22], it follows from (5.4) and (5.7) that

$$\begin{aligned} \dot{\sigma}_{ij} = & \left\{ \bar{\mu}(\delta_{ik}\delta_{jl} + \delta_{il}\delta_{jk}) + \left(\kappa - \frac{2}{3}\bar{\mu} \right) \delta_{ij}\delta_{kl} \right\} D_{kl} + (\mu - \bar{\mu}) \frac{1}{\bar{\sigma}^2} \sigma'_{ij}\sigma'_{kl} D_{kl} \\ & - \frac{1}{H + \mu - 9\kappa} \frac{\partial G}{\partial I} \frac{\partial F}{\partial I} \left\{ \mu \frac{\sigma'_{ij}}{\bar{\sigma}} + 3\kappa \frac{\partial G}{\partial I} \delta_{ij} \right\} \left\{ \mu \frac{\sigma'_{kl}}{\bar{\sigma}} - 3\kappa \frac{\partial F}{\partial I} \delta_{kl} \right\} D_{kl}, \end{aligned} \quad (5.8)$$

where

$$\frac{1}{\bar{\mu}} = \frac{1}{\mu} + 2A. \quad (5.9)$$

For application to plane strain it is required that

$$D_{22} = 0. \quad (5.10)$$

The corresponding plastic part is almost zero if

$$\sigma'_{22} = -2 \frac{\partial G}{\partial I} \bar{\sigma}, \quad (5.10')$$

and if it is assumed that A in (5.7) is negligibly small as compared with $1/H$, which is the case for the present problem as will be shown later on. Then the above equation holds if

$$\begin{aligned} \frac{\sigma'_{11}}{\bar{\sigma}} = \frac{\partial G}{\partial I} + \left(\frac{1 - 3 \left(\frac{\partial G}{\partial I} \right)^2}{1 + t^2} \right), & \quad \frac{\sigma'_{22}}{\bar{\sigma}} = -2 \frac{\partial G}{\partial I}, \\ \frac{\sigma'_{33}}{\bar{\sigma}} = \frac{\partial G}{\partial I} - \left(\frac{1 - 3 \left(\frac{\partial G}{\partial I} \right)^2}{1 + t^2} \right), & \quad \frac{\sigma'_{13}}{\bar{\sigma}} = t \left(\frac{1 - 3 \left(\frac{\partial G}{\partial I} \right)^2}{1 + t^2} \right), \end{aligned} \quad (5.11)$$

where t is defined in (5.13). In the application which follows, this condition is essentially satisfied. The elastic contribution to the l.h.s. of (5.10), in general, does not vanish under condition (5.11), unless the Poisson ratio associated with moduli μ and κ in (5.4) is $1/2$. For application here, it is envisaged that large plastic flows precede localized deformations, and therefore, the corresponding elastic distortion is negligibly small when compared with the

plastic part. In this situation it may be assumed that restriction (5.11) results in a plane strain condition with reasonable accuracy.

With the aid of (5.10) and (5.11) the rate constitutive relations (5.8) reduce to

$$\begin{aligned}\dot{\sigma}_{11} &= a_1 D_{11} + 2a_2 D_{13} + a_3 D_{33}, \\ \dot{\sigma}_{33} &= b_1 D_{11} + 2b_2 D_{13} + b_3 D_{33}, \\ \dot{\sigma}_{13} &= c_1 D_{11} + 2c_2 D_{13} + c_3 D_{33},\end{aligned}\quad (5.12)$$

and upon the introduction of quantities,

$$\begin{aligned}t &= \frac{\sigma_{13}}{\tau}, & \tau &= \frac{1}{2}(\sigma_{11} - \sigma_{33}), \\ \alpha &= -3 \frac{\partial F}{\partial I}, & \beta &= 3 \frac{\partial G}{\partial I}, \\ \bar{h} &= H + \mu + \kappa\alpha\beta, & g &= \sqrt{\left(\frac{1 - \beta^2/3}{1 + t^2}\right)}, \\ e &= \frac{1}{3}\beta + g, & f &= \frac{1}{3}\beta - g, \\ a &= \mu e + \kappa\beta, & b &= \mu e + \kappa\alpha, \\ c &= \mu f + \kappa\beta, & d &= \mu f + \kappa\alpha,\end{aligned}\quad (5.13)$$

the following explicit expressions are obtained for the parameters in (5.12):

$$\begin{aligned}a_1 &= \left(\kappa + \frac{4}{3}\bar{\mu}\right) + (\mu - \bar{\mu})e^2 - ab/\bar{h}, \\ a_2 &= (\mu - \bar{\mu})etg - at\mu g/\bar{h}, \\ a_3 &= \left(\kappa - \frac{2}{3}\bar{\mu}\right) + (\mu - \bar{\mu})ef - ad/\bar{h}, \\ b_1 &= \left(\kappa - \frac{2}{3}\bar{\mu}\right) + (\mu - \bar{\mu})ef - cb/\bar{h}, \\ b_2 &= (\mu - \bar{\mu})ftg - ct\mu g/\bar{h}, \\ b_3 &= \left(\kappa + \frac{4}{3}\bar{\mu}\right) + (\mu - \bar{\mu})f^2 - cd/\bar{h}, \\ c_1 &= (\mu - \bar{\mu})etg - bt\mu g/\bar{h}, \\ c_2 &= \bar{\mu} + (\mu - \bar{\mu})t^2g^2 - \mu^2t^2g^2/\bar{h}, \\ c_3 &= (\mu - \bar{\mu})ftg - dt\mu g/\bar{h}.\end{aligned}\quad (5.14)$$

6. LOCALIZATION

In the calculation of localization of deformation the inception of the localized flow is taken to coincide with conditions under which real characteristics for the corresponding rate field equations develop. The necessary condition then is the continuity of the traction rates across the discontinuity surfaces. If ν is a unit vector defining the orientation of such a surface, it must be required that

$$\langle \dot{\tau}_{ij} \rangle \nu_j = 0, \quad j, i = 1, 3, \quad (6.1)$$

where the nominal stress rate $\dot{\tau}_{ij}$ is given by

$$\dot{\tau}_{ij} = \dot{\sigma}_{ij} - D_{ik}\sigma_{kj} + W_{ik}\sigma_{kj} + D_{kk}\sigma_{ij}, \quad (6.2)$$

and where $\langle f \rangle$ denotes the jump in the value of f across the discontinuity surface. The corresponding jump in the velocity gradient is,

$$\langle v_{i,j} \rangle = \eta_i \nu_j, \quad (6.3)$$

where η_i is the corresponding jump; both η and ν are functions of the spatial coordinates in a nonhomogeneous deformation field.

With the aid of eqns (5.10), (5.11), (6.3) and constitutive relations (5.12), continuity relations (6.1) yield a system of two homogeneous linear equations for the jump magnitudes η_1 and η_3 ; $\eta_2 \equiv 0$ in plane strain. Non-trivial solutions exist if the determinant of the coefficients vanishes. This leads to the characteristic equation defining inception of localization,

$$\begin{aligned} & [(a_1 c_2 - c_1 a_2) + \tau(a_1 + t c_1)](\nu_1)^4 \\ & + [(a_1 b_2 - b_1 a_2 + a_1 c_3 - c_1 a_3) + \tau\{2a_2 + t(a_1 + b_1 + 2c_2)\}](\nu_1)^3 \nu_3 \\ & + [(a_1 b_3 - b_1 a_3 + c_1 b_2 - b_1 c_2 + a_2 c_3 - c_2 a_3) \\ & + \tau\{(a_3 - b_1) + t(2b_2 + 2a_2 + c_1 + c_3)\}](\nu_1)^2 (\nu_3)^2 \\ & + [(a_2 b_3 - b_2 a_3 + c_1 b_3 - b_1 c_3) - \tau\{2b_2 - t(a_3 + b_3 + 2c_2)\}]\nu_1 (\nu_3)^3 \\ & + [(b_3 c_2 - c_3 b_2) - \tau(b_3 - t c_3)](\nu_3)^4 = 0. \end{aligned} \quad (6.4)$$

The current stress distribution in the necked region of the bar is given in Section 3. Therefore, the coefficients (5.14) can be calculated by direct substitution. One hence seeks at each point within the necked region the minimum value of σ_0 , which, for the first time, provides real characteristics for (6.4). Since the parameter τ in (5.13) is proportional to σ_0 , (6.4) yields

$$\tau = \tau_n / \tau_d, \quad (6.5)$$

where

$$\begin{aligned} \tau_n &= (a_2 c_1 - c_2 a_1) \chi^4 + (a_2 b_1 - b_2 a_1 + c_1 a_3 - a_1 c_3) \chi^3 \\ &+ (b_1 a_3 - a_1 b_3 + c_2 b_1 - b_2 c_1 + c_2 a_3 - a_2 c_3) \chi^2 \\ &+ (b_2 a_3 - a_2 b_3 + c_3 b_1 - c_1 b_3) \chi + (c_3 b_2 - b_3 c_2), \\ \tau_d &= (a_1 + t c_1) \chi^4 + \{2a_2 + t(a_1 + b_1 + 2c_2)\} \chi^3 \\ &+ \{(a_3 - b_1) + t(2b_2 + 2a_2 + c_1 + c_3)\} \chi^2 \\ &- \{2b_2 - t(a_3 + b_3 + 2c_2)\} \chi - (b_3 - t c_3), \end{aligned} \quad (6.6)$$

and where

$$\chi = \nu_1 / \nu_3. \quad (6.7)$$

One then minimizes τ with respect to χ , to arrive at a polynomial of degree six in χ . The values of χ so obtained provide extremes of σ_0 , the smallest of which is the critical stress, the corresponding χ defining the inclination of the shear band.

7. NUMERICAL RESULTS AND DISCUSSION

In this section specific numerical results are obtained and compared with some existing experimental observations. Attention is confined to the case of uniaxial extension, and parameters in the rate constitutive relations (5.8) and in the expression for the necked profile are specified by the consideration of experimental results. Then the minimum value of τ and the corresponding characteristic directions are calculated at each point in the necked region. This calculation is guided by the experimental results of Anand and Spitzig[2], who report diffused necking to occur at axial strain of $\epsilon_1 = 0.029$ and localized shear bands at $\epsilon_1 = 0.034$. From (4.5)

and (4.6), therefore,

$$\lambda_t = 1.034 = 1.029 \frac{1}{1 - \zeta - \xi}, \quad (7.1)$$

and hence

$$\zeta + \xi = 0.00484. \quad (7.2)$$

To compare results with the numerical calculations of Tvergaard *et al.*[3], consider the following four specific cases:

$$\begin{aligned} \text{I: } & \zeta = 0.00484, & \xi &= 0, \\ \text{II: } & \zeta = 0.00334, & \xi &= 0.0015, \quad n = 2, \\ \text{III: } & \zeta = 0.00334, & \xi &= 0.0015, \quad n = 3, \\ \text{IV: } & \zeta = 0.00634, & \xi &= -0.0015, \quad n = 4, \end{aligned} \quad (7.3)$$

and choose $H_0/l = 2/3$.

Since little information on dilatancy and pressure-sensitivity is available, the parameters $\partial G/\partial I$ and $\partial F/\partial I$ must be fixed somewhat arbitrarily. Their ranges of variation, however, at least for some high strength steels, can be fixed from the experimental results of Spitzig *et al.*[23, 24], i.e.

$$0 \leq 3 \frac{\partial G}{\partial I} \leq 0.01, \quad 0 \leq -3 \frac{\partial F}{\partial I} \leq 0.1. \quad (7.4)$$

Furthermore, assume that μ and κ are the usual elastic moduli, set

$$\nu = 0.3, \quad (7.5)$$

and obtain, using the data of Anand and Spitzig[2], i.e. Young's modulus of $E = 207 \text{ GPa}$,

$$\frac{\kappa}{\mu} = \frac{2(1 + \nu)}{3(1 - 2\nu)} = 2.1667, \quad (7.6)$$

$$\mu = \frac{E}{2(1 + \nu)} = 79,600 \text{ MPa}. \quad (7.7)$$

To fix parameters A and H in the rate constitutive relations, or at least their order of magnitude, consider the limiting case,

$$\kappa \rightarrow \infty, \quad \frac{\partial G}{\partial I} \rightarrow 0, \quad \text{and} \quad \frac{\partial F}{\partial I} \rightarrow 0, \quad (7.8)$$

which results in

$$D_{ij} = \left(\frac{1}{2\mu} + A \right) \dot{\sigma}'_{ij} + \left(\frac{1}{2H} - A \right) \frac{\sigma'_{ij} \sigma'_{kl}}{2\sigma'^2} \dot{\sigma}'_{kl}. \quad (7.9)$$

Comparison of (7.9) with the *deformation* theory model of Stören and Rice[7], namely,

$$D_{ij} = \frac{1}{2h_1} \dot{\sigma}'_{ij} + \left(\frac{1}{2h} - \frac{1}{2h_1} \right) \frac{\sigma'_{ij} \sigma'_{kl}}{2\sigma'^2} \dot{\sigma}'_{kl}, \quad (7.10)$$

shows that

$$\frac{1}{h_1} = \frac{1}{2\mu} + A, \quad \frac{1}{h} = \frac{1}{2H} + \frac{1}{2\mu}, \quad (7.11)$$

where h_1 and h respectively are the secant and tangent moduli in the effective stress, effective strain-relation, i.e. in the $\bar{\sigma}$, $\bar{\epsilon}$ -curve. Since in the present case,

$$\bar{\sigma} = \frac{1}{2} \sigma_0, \quad \bar{\epsilon} = 2\epsilon_1, \quad (7.12)$$

where ϵ_1 is the elongation in the x_1 -direction, it follows that

$$h_1 = \frac{\bar{\sigma}}{\bar{\epsilon}} = \frac{1}{4} \frac{\sigma_0}{\epsilon_1}, \quad h = \frac{d\bar{\sigma}}{d\bar{\epsilon}} = \frac{1}{4} \frac{d\sigma_0}{d\epsilon_1}. \quad (7.13)$$

Experimental results of Anand and Spitzig[2] now yield

$$4h_1 = 58,656 \text{ MPa}, \quad 4h = 391 \text{ MPa}, \quad (7.14)$$

at the inception of shear bands. Also, from (7.7) and (7.11),

$$\frac{\bar{\mu}}{\mu} = \frac{1}{1 + 2\mu A} = 0.092, \quad \frac{H}{\mu} = 0.00061, \quad (7.15)$$

which hold only at the incipience of localization.

The corresponding numerical results obtained from characteristic condition (6.5) for the minimum value of stress, σ_0 , and the corresponding localization orientation are summarized in Table 1. Since in the experiments it is found that

$$\sigma_0 \approx 1,900 \sim 2,000 \text{ MPa}, \quad \theta = \pm(38 \pm 2)^\circ, \quad (7.16)$$

at the critical state, the results in Table 1 are not in good accord with experiments. In Table 1, sensitivity of the results to the variation in the parameters β and α , i.e. the dilatancy and pressure-sensitivity, is also displayed. However, these factors do not seem to be of major importance within the realistic ranges of their variation defined by (7.4).

The results are, however, highly sensitive to the variation of the noncoaxiality parameter A (or $\bar{\mu}$) and the work-hardening parameter H . In general, there is no reason to associate parameter A directly with the secant compliance, as is suggested by (7.13). Only by special considerations does such association become meaningful; see Stören and Rice[7]. Therefore,

Table 1. Critical stress (numbers in parentheses in MPa) and shear band orientation for $\bar{\mu}/\mu = 0.092$, $H/\mu = 0.00061$ and indicated values of α and β

Case Eqn. (7.3)	$\alpha = \beta = 0$		$\alpha = 0.1, \beta = 0$		$\alpha = 0, \beta = 0.01$		$\alpha = 0.1, \beta = 0.01$	
	σ_0/μ	θ	σ_0/μ	θ	σ_0/μ	θ	σ_0/μ	θ
I	0.0296 (2360)	± 42.6	0.0121 (963)	± 45.4	0.0313 (2490)	± 42.6	0.0139 (1110)	± 45.4
II	0.0297 (2360)	42.7 -42.5	0.0121 (963)	45.5 -45.4	0.0314 (2500)	42.7 -42.5	0.0139 (1110)	45.5 -45.4
III	0.0297 (2360)	42.2 -43.0	0.0121 (963)	45.0 -45.9	0.0314 (2500)	42.2 -43.0	0.0139 (1110)	45.0 -45.9
IV	0.0293 (2330)	± 42.6	0.0120 (955)	± 45.4	0.0311 (2480)	± 42.6	0.0137 (1090)	± 45.4

the values of α , β and κ/μ are fixed at

$$\alpha = 0.1, \quad \beta = 0.01, \quad \kappa/\mu = 2.1667, \tag{7.17}$$

and, for several values of A (or $\bar{\mu}$) and H , critical values of σ_0 and shear band orientation are obtained. Table 2 presents the corresponding results which show that the smaller values of $\bar{\mu}/\mu$ are required in order to obtain critical values in good accord with experimental observation; see also Fig. 2.

This suggests that the incipience of shear band formation is marked at a stage of deformation which is essentially incompressible, and that locally, the value of $\bar{\mu}/\mu$ is very small at the point where the band first occurs. To check this statement we set

$$\alpha = \beta = 0, \quad \frac{\kappa}{\mu} = 2.1667, \\ 0.1 > \frac{\bar{\mu}}{\mu} \geq 0.01, \quad 0.002 \geq \frac{H}{\mu} \geq 0.00061, \tag{7.18}$$

and calculate the critical values of σ_0/μ and θ as shown in Fig. 3 for Case I. From this figure it follows that experimental results are confirmed with the following values of the parameters:

$$\alpha = \beta = 0, \quad \frac{\kappa}{\mu} = 2.1667, \\ \frac{\bar{\mu}}{\mu} = 0.028, \quad \frac{H}{\mu} = 0.0015. \tag{7.19}$$

The corresponding results are shown in Table 3. Figure 4 gives for the indicated cases, the contours of the minimum (critical) values of σ_0/μ , when ellipticity is lost. In other words, each contour line associated with the indicated stress level, separates the region in which the governing equations are elliptic (below the contour line) from that in which the equations are

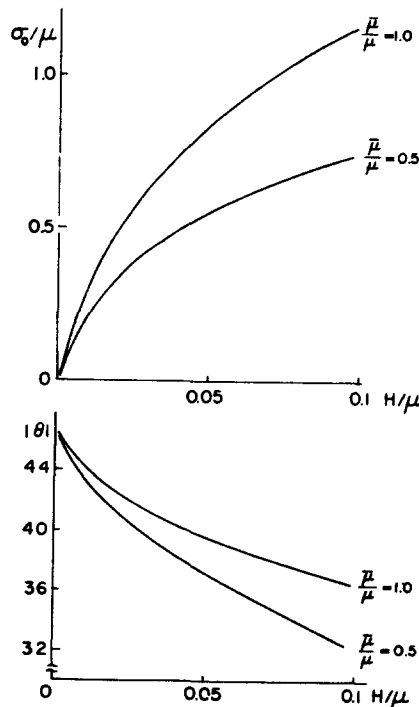


Fig. 2. Critical values of axial stress and localization direction for various values of $\bar{\mu}/\mu$ and H/μ ; Case I with $\alpha = 0.1$, $\beta = 0.01$ and $\kappa/\mu = 2.1667$.

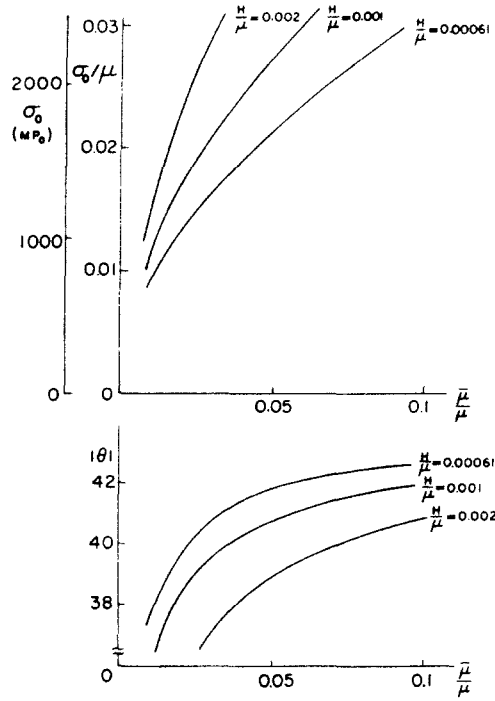


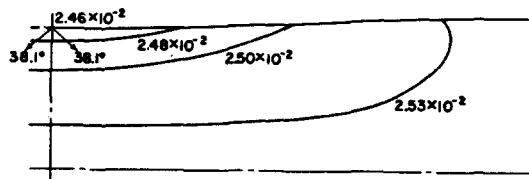
Fig. 3. Critical values of axial stress and localization direction for various values of $\bar{\mu}/\mu$ and H/μ ; Case I with $\alpha = \beta = 0$ and $\kappa/\mu = 2.1667$.

Table 2. Critical stress and shear band orientation for $\alpha = 0.1$, $\beta = 0.01$, $\kappa/\mu = 2.1667$ and indicated values of $\bar{\mu}/\mu$ and H/μ

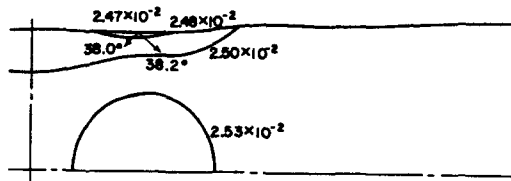
$\frac{\bar{\mu}}{\mu}$	$\frac{H}{\mu}$	σ_0/μ (θ)			
		Case I	Case II	Case III	Case IV
1.0	0.01	0.307 (± 44.1)	0.308 ($\begin{smallmatrix} 44.2 \\ -44.0 \end{smallmatrix}$)	0.308 ($\begin{smallmatrix} 43.7 \\ -44.5 \end{smallmatrix}$)	0.304 (± 44.1)
	0.03	0.629 (± 41.5)	0.631 ($\begin{smallmatrix} 41.6 \\ -41.5 \end{smallmatrix}$)	0.631 ($\begin{smallmatrix} 41.1 \\ -42.0 \end{smallmatrix}$)	0.623 (± 41.5)
	0.05	0.836 (± 39.8)	0.838 ($\begin{smallmatrix} 39.8 \\ -39.7 \end{smallmatrix}$)	0.838 ($\begin{smallmatrix} 39.3 \\ -40.2 \end{smallmatrix}$)	0.828 (± 39.8)
	0.07	0.992 (± 38.3)	0.995 ($\begin{smallmatrix} 38.4 \\ -38.2 \end{smallmatrix}$)	0.995 ($\begin{smallmatrix} 37.8 \\ -38.7 \end{smallmatrix}$)	0.984 (± 38.3)
	0.09	1.12 (± 37.0)	1.12 ($\begin{smallmatrix} 37.1 \\ -36.9 \end{smallmatrix}$)	1.12 ($\begin{smallmatrix} 36.5 \\ -37.4 \end{smallmatrix}$)	1.11 (± 37.0)
0.5	0.001	0.0145 (± 46.3)	0.0146 ($\begin{smallmatrix} 46.4 \\ -46.2 \end{smallmatrix}$)	0.0146 ($\begin{smallmatrix} 45.8 \\ -46.7 \end{smallmatrix}$)	0.0144 (± 46.3)
	0.01	0.220 (± 43.2)	0.221 ($\begin{smallmatrix} 43.3 \\ -43.1 \end{smallmatrix}$)	0.221 ($\begin{smallmatrix} 42.7 \\ -43.6 \end{smallmatrix}$)	0.218 (± 43.2)
	0.03	0.427 (± 39.7)	0.428 ($\begin{smallmatrix} 39.8 \\ -39.6 \end{smallmatrix}$)	0.428 ($\begin{smallmatrix} 39.3 \\ -40.1 \end{smallmatrix}$)	0.423 (± 39.7)
	0.05	0.556 (± 37.2)	0.557 ($\begin{smallmatrix} 37.3 \\ -37.1 \end{smallmatrix}$)	0.557 ($\begin{smallmatrix} 36.7 \\ -37.6 \end{smallmatrix}$)	0.551 (± 37.2)
	0.07	0.650 (± 35.0)	0.651 ($\begin{smallmatrix} 35.1 \\ -34.9 \end{smallmatrix}$)	0.651 ($\begin{smallmatrix} 34.5 \\ -35.4 \end{smallmatrix}$)	0.644 (± 35.0)
	0.09	0.722 (± 33.0)	0.724 ($\begin{smallmatrix} 33.1 \\ -32.9 \end{smallmatrix}$)	0.724 ($\begin{smallmatrix} 32.5 \\ -33.4 \end{smallmatrix}$)	0.716 (± 33.0)

Table 3. Critical stress and shear band orientation for $\alpha = \beta = 0$, $\kappa/\mu = 2.1667$, $\bar{\mu}/\mu = 0.028$ and $H/\mu = 0.0015$

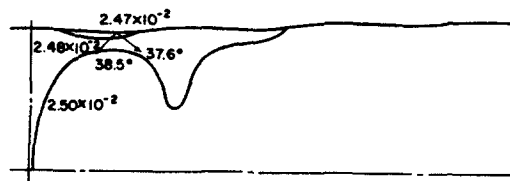
Case Equ. (7.3)	σ_0/μ	σ_0 (MPa)	θ
I	2.46×10^{-2}	1960	± 38.1
II	2.47×10^{-2}	1970	38.2 -38.0
III	2.47×10^{-2}	1970	37.6 -38.5
IV	2.44×10^{-2}	1940	± 38.1



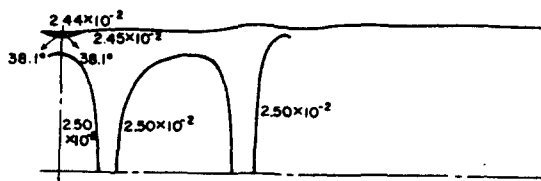
CASE I



CASE II



CASE III



CASE IV

Fig. 4. Contours of critical values of σ_0/μ for four different neck profiles; $\alpha = \beta = 0$, $\kappa/\mu = 2.1667$, $\bar{\mu}/\mu = 0.028$ and $H/\mu = 0.0015$ (the variation of neck profile exaggerated).

Table 4. Critical stress and shear band orientation for $\alpha = \beta = 0$, $\kappa/\mu = 2.1667$, $H/\mu = 0.0015$ and indicated values of $\bar{\mu}/\mu$

Case Eqn. (7.3)	$\bar{\mu} = 0.028$ μ ($A=2.18 \times 10^{-4} \text{ MPa}^{-1}$) σ_0/μ (θ)	$\bar{\mu} = 1.0$ μ ($A \equiv 0$) (θ)
I	2.46×10^{-2} (± 38.1)	1.78×10^{-1} (± 43.7)
II	2.47×10^{-2} $\begin{pmatrix} 38.2 \\ -38.0 \end{pmatrix}$	1.78×10^{-1} $\begin{pmatrix} 43.8 \\ -43.6 \end{pmatrix}$
III	2.47×10^{-2} $\begin{pmatrix} 37.6 \\ -38.5 \end{pmatrix}$	1.78×10^{-1} $\begin{pmatrix} 43.2 \\ -44.1 \end{pmatrix}$
IV	2.44×10^{-2} (± 38.1)	1.76×10^{-1} (± 43.7)
V ($H = H_0$)	2.53×10^{-2} (± 38.1)	1.83×10^{-1} (± 43.7)

hyperbolic (above the contour line). On the contour line, therefore, the governing equations are parabolic.

For the point in the necked region where shear bands first occur (i.e. for the smallest σ_0/μ), the directions of the bands are also indicated. As is seen this location is highly dependent on the neck profile, as has also been verified numerically by Tvergaard *et al.* [3]. The stress distribution changes (from that defined by (3.11)) after the inception of shear bands, and continues to change as the bands grow. Hence the exact evolution of the shear bands cannot be decided from the results presented in Fig. 4. However, these results do suggest a reasonable shear band growth pattern which is in good qualitative agreement with the numerical results presented by Tvergaard *et al.* [3]. In Case I the bands first are initiated at the free surface and at the middle of the necked region, and then, as suggested by the corresponding contour lines, propagate into the specimen, the initial angle being $\pm 38^\circ$. In Case II, on the other hand, the bands are formed again at the surface, but off-center. Similar results are displayed for Cases III and IV.

We have also calculated the corresponding results for a different state of stress at infinity from that corresponding to (3.11). In (3.11), σ_{11} is uniform at $x_1 = \pm l$, and σ_{33} does not vanish identically there. A different loading condition is possible where $\sigma_{33}(\pm l) = 0$, in which case σ_{11} at $x_1 = \pm l$ will not be uniform, and will depend on x_3 . The calculation is similar to the case presented above, but the location of the shear band initiation in certain cases may move into the interior of the necked region. Since experiments suggest both possibilities, the actual loading mechanism should enter in the calculation of the shear band initiation in a necked bar.

To show that only the location of the shear band, and not the critical load, is sensitive to the variation in the neck profile, a constant profile of $H \equiv H_0$ is used together with the values of parameters given by (7.19). The resulting critical stress then is $\sigma_0 \approx 2010$ MPa, with shear band orientation of $\theta = \pm 38^\circ$, the critical stress being slightly higher than the observed one. On the other hand, the noncoaxiality parameter, A , has a significant effect on the critical value of stress. This is shown in Table 4 when results for $A = 2.18 \times 10^{-4} \text{ MPa}^{-1}$ and $A \equiv 0$ are compared for different neck profiles, including the case of $H \equiv H_0$.

Acknowledgements—This work has been supported by the National Science Foundation under Grant No. ENG 76-03921 to Northwestern University.

REFERENCES

1. P. F. Weinrich and I. E. French, The influence of hydrostatic pressure on the fracture mechanisms of sheet tensile specimens of copper and brass. *Acta Met.* **24**, 317 (1976).
2. L. Anand and W. A. Spitzig, Initiation of localized shear bands in plane strain. *J. Mech. Phys. Solids* **28**, 113 (1980).
3. V. Tvergaard, A. Needleman and K. K. Lo, Flow localization in the plane strain tensile test. *Materials Res. Laboratory Techn. Rep. No. MRL E-123*, Division of Engineering, Brown University, Providence, R. I. *J. Mech. Phys. Solids* **29**, 115 (1981).
4. R. Hill, Acceleration waves in solids. *J. Mech. Phys. Solids* **10**, 1 (1962).
5. R. Hill and J. W. Hutchinson, Bifurcation phenomena in the plane tension test. *J. Mech. Phys. Solids* **23**, 239 (1975).
6. J. R. Rice, The localization of plastic deformation. *Proc. 14th Int. Congr. of Theoretical and Appl. Mech.* **1**, 207 (1976).

7. S. Stören and J. R. Rice, Localized necking in thin sheets. *J. Mech. Phys. Solids* **23**, 421 (1975).
8. J. W. Rudnicki and J. R. Rice, Conditions for the localization of deformation in pressure-sensitive dilatant materials. *J. Mech. Phys. Solids* **23**, 371 (1975).
9. J. W. Hutchinson and K. W. Neale, Sheet necking—II. Time-independent behavior. *Mechanics of Sheet Metal Forming* (Edited by D. P. Koistinen and N.-M. Wang), Plenum Press New York, 127 (1978).
10. J. K. Knowles and E. Sternberg, On the ellipticity of the equations of nonlinear elastostatics for a special material. *J. Elasticity* **5**, 341 (1975).
11. A. Needleman, Non-normality and bifurcation in plane strain tension and compression. *J. Mech. Phys. Solids* **27**, 231 (1979).
12. S. Nemat-Nasser, Finite deformation plasticity and plastic instability. *Trans. 25th Conf. Army Mathematicians* 715 (1979).
13. S. Nemat-Nasser and A. Shokooh, On finite plastic flows of compressible materials with internal friction. *Int. J. Solids Structures* **16**, 495 (1980).
14. J. Christoffersen and J. W. Hutchinson, A class of phenomenological corner theories of plasticity. *Techn. Rep. No. MECH-8*, Division of Applied Sciences, Harvard University, Cambridge, Mass. (Jan. 1979); *J. Mech. Phys. Solids* **27**, 465 (1979).
15. J. Mandel, Sur les lignes de glissement et le calcul des déplacements dans la déformation plastique. *Comptes rendus de l'Académie des Sciences* **225**, 1272 (1947).
16. A. J. M. Spencer, A theory of the kinematics of ideal soils under plane strain conditions. *J. Mech. Phys. Solids* **12**, 337 (1964).
17. A. J. M. Spencer, Deformation of ideal granular materials. *Mechanics of Solids*, The Rodney Hill 60th Anniversary Volume (Edited by H. G. Hopkins and M. J. Sewell), Pergamon Press, Oxford, to appear.
18. M. M. Mehrabadi and S. C. Cowin, Initial planar deformation of dilatant granular materials. *J. Mech. Phys. Solids* **26**, 269 (1978).
19. M. M. Mehrabadi and S. C. Cowin, Pre-failure and post-failure soil plasticity models. *J. Engr. Mech. Div., Trans. ASCE*, **106**, 991 (1980).
20. J. Christoffersen, M. M. Mehrabadi and S. Nemat-Nasser, A micromechanical description of granular material behavior. *Earthquake Research and Engineering Laboratory Technical Report No. 80-1-22*, Dept. of Civil Engng, Northwestern University, Evanston, Ill. (Jan. 1980); *J. Appl. Mech.* **48**, 339 (1981).
21. S. Nemat-Nasser, M. M. Mehrabadi and T. Iwakuma, On certain macroscopic and microscopic aspects of plastic flow of ductile materials. *Three-Dimensional Constitutive Relations and Ductile Fracture*, Proc. IUTAM Symp., Dourdan, France, 2-5 June, 1980 (Edited by S. Nemat-Nasser), North-Holland, Amsterdam 151 (1981).
22. S. Nemat-Nasser, Decomposition of strain measures and their rates in finite deformation elastoplasticity. *Int. J. Solids Structures* **15**, 155 (1979).
23. W. A. Spitzig, R. J. Sober and O. Richmond, Pressure dependence of yielding and associated volume expansion in tempered martensite. *Acta Met.* **23**, 885 (1975).
24. W. A. Spitzig, R. J. Sober and O. Richmond, The effect of hydrostatic pressure on the deformation behavior of maraging and HY-80 steels and its implication for plasticity theory. *Met. Trans. A* **7A**, 1703 (1976).